18–20°). The spreading of the halo prevents an accurate evaluation of the average lateral distance, and consequently we could not determine whether the ligand or the counterion influences these distances. Furthermore, scattering at wide angles is related to some average electron density distribution, which originates from different interferences (between silver atoms, paraffinic chains aromatic groups, counterions). The effect on the X-ray pattern of an eventual separation of the rigid cores of neighboring molecules would be masked by a higher degree of chain melting, as it is not possible to differentiate between the contribution of the chains and of the rest of the molecule to X-ray diffraction.

Acknowledgment. We express our appreciation to Dr. A. M. Levelut (Laboratoire de Physique des Solids, University Paris-Sud) for providing access to the X-ray equipment. Likewise, Dr. J. Barberá acknowledges a NATO grant. This work was supported by the EEC (Project ST2J-0387-C).

Registry No. L^1 (n = 1), 129985-68-8; L^1 (n = 2), 129985-69-9; L^1 (n = 3), 129985-70-2; L^1 (n = 4), 129985-71-3; L^1 (n = 5), 129985-72-4; L^1 (n = 6), 129985-73-5; L^1 (n = 7), 129985-74-6; L^1 (n = 8), 129985-75-7; L^1 (n = 9), 129985-76-8; L^1 (n = 10), 129985-77-9; L^1 (n = 12), 129985-78-0; L^1 (n = 14), 129985-79-1; L^1 (n = 16), 129985-80-4; L^2 (n = 2), 129985-81-5; L^2 (n = 4), 129985-82-6; L^2 (n = 6), 129985-83-7; L^2 (n = 10), 129985-84-8; L^2 (n = 14), 129985-85-9; $[AgL^1{}_2]^+BF_4^-$ (n = 1), 130010-99-0; $[AgL^1{}_2]^+BF_4^-$ (n = 2), 122676-75-9; $[AgL^1{}_2]^+BF_4^-$ (n = 3), 130011-01-7; $[AgL^1{}_2]^+BF_4^-$ (n = 4), 130011-03-9; $[AgL^1{}_2]^+BF_4^-$ (n = 5), 130011-05-1; $[AgL^1{}_2]^+BF_4^-$ (n = 6), 130011-07-3; $[AgL^1{}_2]^+BF_4^-$ (n = 7), 130011-09-5; $[AgL^1{}_2]^+BF_4^-$ (n = 8), 130011-11-9; $[AgL^1{}_2]^+BF_4^-$ (n = 9), 130011-13-1; $[AgL^1{}_2]^+BF_4^-$ (n = 10), 130011-15-3; $[AgL^1{}_2]^+BF_4^-$ (n = 12), 130011-17-5; $[AgL^1{}_2]^+BF_4^-$ (n = 14), 130031-55-9; $[AgL^1{}_2]^+BF_4^-$ (n = 16), 130031-57-1; $[AgL^1{}_2]^+CF_3SO_3^-$ (n = 5), 130011-18-6; $[AgL^1{}_2]^+CF_3SO_3^-$ (n = 6), 130011-19-7; $[AgL^1{}_2]^+CF_3SO_3^-$ (n = 7), 130011-20-0; $[AgL^1{}_2]^+$-$CF_3SO_3^-$ (n = 8), 130011-21-1; $[AgL^1{}_2]^+CF_3SO_3^-$ (n = 9), 130011-22-2; $[AgL^1{}_2]^+CF_3SO_3^-$ (n = 10), 130011-23-3; $[AgL^1{}_2]^+$-$CF_3SO_3^-$ (n = 12), 130011-24-4; $[AgL^1{}_2]^+CF_3SO_3^-$ (n = 14), 130031-58-2; $[AgL^1{}_2]^+CF_3SO_3^-$ (n = 16), 130031-59-3; $[AgL^2{}_2]^+BF_4^-$ (n = 2), 130011-26-6; $[AgL^2{}_2]^+BF_4^-$ (n = 4), 130011-28-8; $[AgL^2{}_2]^+BF_4^-$ (n = 6), 130011-30-2; $[AgL^2{}_2]^+BF_4^-$ (n = 10), 130011-32-4; $[AgL^2{}_2]^+BF_4^-$ (n = 14), 130011-34-6; $[AgL^2{}_2]^+CF_3SO_3^-$ (n = 4), 130011-35-7; $[AgL^2{}_2]^+CF_3SO_3^-$ (n = 6), 130031-60-6; $[AgL^2{}_2]^+CF_3SO_3^-$ (n = 10), 130011-36-8; $[AgL^2{}_2]^+CF_3SO_3^-$ (n = 14), 130011-37-9; $[AgL^1{}_2]^+NO_3^-$ (n = 6), 130011-38-0; $[AgL^1{}_2]^+PF_6^-$ (n = 6), 130011-39-1.

Low-Dimensional Organometallic Electron-Transfer Complexes. X-ray Structures and Magnetic Properties of α- and β-$[Cr(C_6Me_3H_3)_2]^{\bullet+}[TCNQ]^{\bullet-}$

Dermot O'Hare,[1a] Michael D. Ward,*[,1b] and Joel S. Miller*

Central Research and Development Department,† E. I. du Pont de Nemours and Company,
Experimental Station E328, Wilmington, Delaware 19880-0328

Received May 14, 1990

The reaction of donor, $Cr(arene)_2$ (arene = C_6Me_6 and $C_6Me_3H_3$), D, with the acceptor TCNQ, A, results in formation of electron-transfer salts of $[D]^{\bullet+}[A]^{\bullet-}$ composition. Two phases of $[Cr(C_6Me_3H_3)_2]^{\bullet+}[TCNQ]^{\bullet-}$ have been structurally characterized. The α-phase belongs to the centrosymmetric $C2/c$ space group [a = 14.014 (4) Å, b = 16.347 (4) Å, c = 22.964 (6) Å, β = 107.44 (2)°, Z = 8, V = 5019 (5) Å^3, T = 23 °C, R = 0.082] with the solid-state structure consisting of $\cdots D^{\bullet+}D^{\bullet+}A_2{}^{2-}D^{\bullet+}D^{\bullet+}\cdots$ linear chains. Each $[TCNQ]^-$ in the $[TCNQ]_2{}^{2-}$ dimer is planar, and the intradimer separation is 3.47 Å. The anion–anion overlap is unusual as the dihedral angle between the planes normal to the long molecular axes is 31°. The β-phase crystallizes in the $P2_1/c$ space group [a = 9.588 (5) Å, b = 16.390 (3) Å, c = 8.419 (6) Å, β = 106.84 (6)°, Z = 2, V = 1266 (9) Å^3, T = 23 °C, R = 0.044] with the solid-state structure consisting of $\cdots D^{\bullet+}A^{\bullet-}D^{\bullet+}A^{\bullet-}\cdots$ linear chains. The magnetic susceptibility of α-$[Cr(C_6Me_6)_2][TCNQ]$ obeys the Curie–Weiss law with an effective moment, μ_{eff}, of 1.77 μ_B and θ of −0.1 K. This is consistent with the presence of a diamagnetic $[TCNQ]_2{}^{2-}$ dimer (ν(C≡N) = 2156 m, 2175 s, and 2182 s cm^{-1}). In contrast, $[Cr(C_6Me_3H_3)_2][TCNQ]$ does not obey the Curie–Weiss law but can be fit to an expression that accounts for contributions from independent Curie spins for the cation and a thermally activated triplet state for the dimerized anions [ΔE = 315 K, 0.027 eV, 219 cm^{-1}, 0.44 kcal/mol].

Introduction

Low-dimensional electron-transfer complexes frequently exhibit unusual optical and electrical properties.[2,3] Recently we reported unusual cooperative magnetic properties for several alternating donor/acceptor electron-transfer complexes.[4] For example, the reaction of $Fe(C_5Me_5)_2$ and TCNQ (TCNQ = 7,7,8,8-tetracyano-p-quinodimethane) gives three products varying in stoichiometry, conductivity, and magnetic properties. The 1-D mixed-stack phase comprising alternating $S = {}^1/_2$ $[Fe(C_5Me_5)_2]^{\bullet+}$ donors and $S = {}^1/_2$ $[TCNQ]^{\bullet-}$ acceptors,[5,6] i.e., $\cdots D^{\bullet+}A^{\bullet-}D^{\bullet+}A^{\bullet-}\cdots$, exhibits a field-dependent metamagnetic switching from an antiferromagnetic to a high moment behavior.[4,7] The structurally similar $[Fe(C_5Me_5)_2]^{\bullet+}[TCNE]^{\bullet-}$ (TCNE =

---

† Contribution no. 5402.

[1] Current address: (a) Department of Inorganic Chemistry, Oxford University, Oxford Oxford, 0X1 3QR, UK. (b) Department of Chemical Engineering and Materials Science, University of Minnesota, Minneapolis, MN 55455.

[2] See for example: *Extended Linear Chain Compounds*; Miller, J. S., Ed.; Plenum: New York; Vols. 1–3. Simon, J.; Andre', J. J. *Molecular Semiconductors*; Springer-Verlag: New York, 1985.

[3] For a detailed overview, see the proceedings of the recent series of international conferences: *Synth. Met.* **1988**, *27*; **1989**, *28*, 29 (Aldissi, M., Ed.); *Mol. Cryst. Liq. Cryst.* **1985**, *117–121* (Pecile, C.; Zerbi, G.; Bozio, R.; Girlando, A., Eds.); *J. Phys. (Paris) Collogue* **1983**, 44-C3 (Comes, R., Bernier, P., Andre', J. J., Rouxel, J., Eds.); *Mol. Cryst. Liq. Cryst.* **1981**, *77, 79, 82, 83, 85*; **1982**, *86* (Epstein, A. J., Conwell, E. M., Eds.); *Chem. Scr.* **1981**, *17* (Carneiro, K., Ed.); *Lect. Notes Phys.* **1979**, *95, 96* (Bartsic, S., Bjelis, A., Cooper, J. R., Leontic, B. A., Eds.); *Ann. N.Y. Acad. Sci.* **1978**, *313* (Miller, J. S., Epstein, A. J., Eds.).

0897-4756/90/2802-0758$02.50/0 © 1990 American Chemical Society

tetracyanoethylene) exhibits bulk ferromagnetism.[4,8,9]

In an effort to elucidate further the structure–function relationships for these electron-transfer salts and to identity their magnetic behavior, we have prepared a series of electron-transfer complexes based on polycyanoanions and group 6A d^5 bisarene radical cations. Since these cations are isoelectronic with $[Fe(C_5Me_5)_2]^{\bullet+}$, direct comparisons of the structural and electronic properties are feasible. The ${}^2E_{2g}$ electronic ground state of the $[Fe(C_5Me_5)_2]^{\bullet+}$[10] leads to large g anisotropies and fast electronic relaxation, which complicate the interpretation of the EPR spectra. Furthermore, due to the g anisotropy the interpretation of powder magnetic susceptibility data is often complicated by alignment effects. In contrast, d^5 bisarene complexes possess ${}^2A_{1g}$ ground states[11] and exhibit room-temperature EPR spectra with little g anisotropy. Hence, the powder magnetic susceptibility data may be more readily interpretable.

An insightful framework to view the stabilization of ferromagnetic coupling in molecular based donor/acceptor complexes is based upon the extended McConnell mechanism.[4b–d,12] Within this model, the stabilization of ferromagnetic coupling arises from the configurational mixing of a charge-transfer excited-state with the ground state. The model predicts that admixture of a nondegenerate donor HOMO with a half-filled nondegenerate acceptor HOMO {as is the case for $[TCNQ]^{\bullet-}$} stabilizes only antiferromagnetic coupling. Since the half-filled ${}^2A_{1g}$ HOMO of $[Cr(arene)_2]^{\bullet+}$ is a nondegenerate orbital, its electron-transfer salts should exhibit antiferromagnetic coupling. Thus, these materials provide a means to test some of these concepts. Structural characterization of the $[Cr^I(arene)_2]^{\bullet+}$ complexes is not very extensive, although the X-ray structure of 1:1 $[Cr^I(C_6H_5Me)_2]^{\bullet+}[TCNQ]^{\bullet-}$, which indicated segregated stacks of cations and anions, has been reported.[13a] The magnetic susceptibilities of $[Cr(C_6H_6)_2]^{\bullet+}[TCNQ]^-$ and $[Cr^I(C_6H_5Me)_2]^{\bullet+}[TCNQ]^-$ were consistent with one unpaired electron per repeat unit. This is attributed to the $S = {}^1/_2$ Cr^I cation and strong antiferromagnetic interactions between $S = {}^1/_2$ $[TCNQ]^{\bullet-}$ anions.[13b] Herein we report on complexes based on $[Cr(C_6Me_6)_2]^{\bullet+}$ and $[TCNQ]^{\bullet-}$; another report has addressed compounds containing $[TCNE]^{\bullet-}$.[14]

Table I. Crystallographic Details for α- and β-$[Cr^I(C_6Me_3H_3)_2][TCNQ]$

	α phase	β phase
formula	$C_{30}H_{28}N_4Cr$	$C_{30}H_{28}N_4Cr$
fw, daltons	496.5	496.5
radiation	Mo Kα	Mo Kα
temp, °C	23	23
space group	$C2/c$	$P2_1/c$
a, Å	14.014 (4)	9.588 (5)
b, Å	16.347 (4)	16.390 (3)
c, Å	22.964 (6)	8.419 (6)
β, deg	107.44 (2)	106.84 (6)
V, Å^3	5019 (5)	1266 (9)
Z	8	2
ρ(calc), g cm^{-3}	1.31	1.3
μ(Mo Kα), cm^{-1}	4.7	4.6
R,[a]	0.082	0.044
R_W,[b]	0.087	0.051

[a] $R = \sum[|F_o| - |F_c|]/\sum|F_o|$. [b] $R_w = [\sum w[|F_o| - |F_c|]^2/\sum w|F_o|^2]^{1/2}$.

Experimental Section

All reactions were performed by using standard Schlenk techniques or in a Vacuum Atmospheres Dri-Lab under a nitrogen atmosphere. EPR spectra were recorded on an IBM/Bruker ER 200 D-SRC spectrometer. Magnetic susceptibility data were recorded by using the Faraday technique from 3 to 300 K.[15] Infrared spectra were measured on a Nicolet 7199 Fourier spectrometer. Elemental analysis and single crystal X-ray studies were performed by Oneida Research Services, Inc. (Whitesboro, NY). $Cr(C_6Me_xH_{6-x})_2$ (x = 3, 6) were prepared according to the literature route.[11b]

$[Cr(C_6Me_3H_3)_2]^{\bullet+}[TCNQ]^{\bullet-}$, 1. $Cr(C_6Me_3H_3)_2$ (100 mg, 0.34 mmol) was dissolved in 10 mL of THF and added to a solution of TCNQ (43 mg, 0.34 mmol) in 3–4 mL of THF. A blue-green solid precipitated immediately, which was collected by vacuum filtration. The precipitate was extracted with CH_2Cl_2 and then concentrated to 5 mL. After cooling overnight to −25 °C blue crystals of the α-phase, 1 α, formed (115 mg, 70%). Anal. Calcd (Found) for $C_{30}H_{28}N_4Cr$: C, 72.56 (72.26); H, 5.68 (5.68); N, 11.28 (11.41). Infrared (Nujol) ν(C≡N) 2152 and 2175 cm^{-1}. On one occasion cooling of a dilute solution overnight to −25 °C led to the isolation of 5–10 mg of green needles of β phase, 1β, which were collected by vacuum filtration. Several attempts to reproduce the preparation of the β-phase were unsuccessful, and the amount of the β-phase available was insufficient for physical measurements other than single-crystal X-ray analysis.

$[Cr(C_6Me_6)_2]^{\bullet+}[TCNQ]^{\bullet-}$, 2. $Cr(C_6Me_6)_2$ (100 mg, 0.26 mmol) was dissolved in 10 mL of hot THF and added to a solution of TCNQ (34 mg, 0.26 mmol) in 3–4 mL of hot THF, resulting in an immediate formation of a blue-green precipitate. After collection by vacuum filtration the precipitate was extracted with CH_2Cl_2 and cooled overnight at −25 °C to yield blue crystals of 2 (115 mg, 86%). Anal. Calcd (Found) for $C_{36}H_{40}N_4Cr$: C, 74.46 (74.33, 74.28); H, 6.94 (6.68, 6.50); N, 9.65 (9.46, 9.37). Infrared (Nujol) ν(C≡N) 2156 m, 2175 s, and 2182 s cm^{-1}.

X-ray Data Collection, Reduction, Solution, and Refinement. The single-crystal X-ray structures of 1α (blue platelet) and 1β (green needle) were solved in the usual fashion. The key parameters for the data collection, data reduction, solution, and refinement are summarized in Table I.

Both structures were solved by Patterson heavy-atom methods that located the position of the Cr atoms. The remaining atoms were located in succeeding difference Fourier syntheses. Hydrogen atoms were added to the structure factor calculations at their calculated positions, but their positions were not refined. The structure was refined in full-matrix least-squares analysis where the function minimized was $\sum w(|F_o| - |F_c|)^2$. Unit weights were used for all observed reflections. Neutral atom scattering factors were taken from Cromer and Waber.[16a] Anomalous dispersion

---

[4] (a) Miller, J. S.; Epstein, A. J.; Reiff, W. M. *Isr. J. Chem.* **1987**, *27*, 363–373. (b) Miller, J. S.; Epstein, A. J.; Reiff, W. M. *Chem. Rev.* **1988**, *88*, 201–220. (c) Miller, J. S.; Epstein, A. J. *NATO Adv. Stud. Ser. B* **1988**, *168*, 159–174. (d) Miller, J. S.; Epstein, A. J.; Reiff, W. M. *Acc. Chem. Res.* **1988**, *21*, 114–120. (e) Miller, J. S.; Epstein, A. J.; Reiff, W. M. *Science* **1988**, *240*, 40–47.

[5] Miller, J. S.; Reis, A. H., Jr.; Gebert, E.; Ritsko, J. J.; Salaneck, W. R.; Kovnat, L.; Cape, T. W.; Van Duyne, R. P. *J. Am. Chem. Soc.* **1979**, *101*, 7111.

[6] Miller, J. S.; Reiff, W. M.: Zhang, J. H.; Preston, L. D.; Reis, A. H., Jr.; Gebert, E.; Extine, M.; Troup, J.; Dixon, D. A.; Epstein, A. J.; Ward, M. D. *J. Phys. Chem.* **1987**, *91*, 4344–4360.

[7] Candela, G. A.; Swartzendruber, L.; Miller, J. S.; Rice, M. J. *J. Am. Chem. Soc.* **1979**, *101*, 2755.

[8] (a) Miller, J. S.; Calabrese, J. C.; Bigelow, R. W.; Epstein, A. J.; Zhang, R. W.; Reiff, W. M. *J. Chem. Soc., Chem. Commun.* **1986**, 1026–1028. (b) Miller, J. S.; Calabrese, J. C.; Rommelmann, H.; Chittipeddi, S.; Zhang, J. H.; Reiff, W. M.; Epstein, A. J. *J. Am. Chem. Soc.* **1987**, *109*, 769–781.

[9] Chittipeddi, S.; Cromack, K. R.; Miller, J. S. *Phys. Rev. Lett.* **1987**, *58*, 2695.

[10] Duggan, D. M.; Hendrickson, D. N. *Inorg. Chem.* **1975**, *14*, 955–970.

[11] (a) Anderson, S. E.; Drago, R. S. *J. Am. Chem. Soc.* **1970**, *92*, 4244. (b) Anderson, S. E.; Drago, R. S. *Inorg. Chem.* **1972**, *11*, 3564.

[12] McConnell, H. M. *Proc. R. A. Welch Found. Chem. Res.* **1967**, *11*, 144. Miller, J. S.; Epstein, A. J. *J. Am. Chem. Soc.* **1987**, *109*, 3850–3856.

[13] (a) Shibaeva, R. P.; Atovmyan, L. O.; Rozenberg, *J. Chem. Soc., Chem. Commun.* **1969**, 649–650. (b) Zvarykina, A. V.; Karimov, Yu. S.; Ljubovsky, R. B.; Makova, M. K.; Khidekel, M. L.; Shchogelov, I. F.; Yagubsky, E. B. *Mol. Cryst. Liq. Cryst.* **1970**, *11*, 217–228.

[14] Miller, J. S.; O'Hare, D. M.; Chackraborty, A.; Epstein, A. J. *J. Am. Chem. Soc.* **1989**, *111*, 7853–7860.

[15] Miller, J. S.; Dixon, D. A.; Calabrese, J. C.; Vazquez, C.; Krusic, P. J.; Ward, M. D.; Wasserman, E.; Harlow, R. L. *J. Am. Chem. Soc.* **1990**, *112*, 381–398.

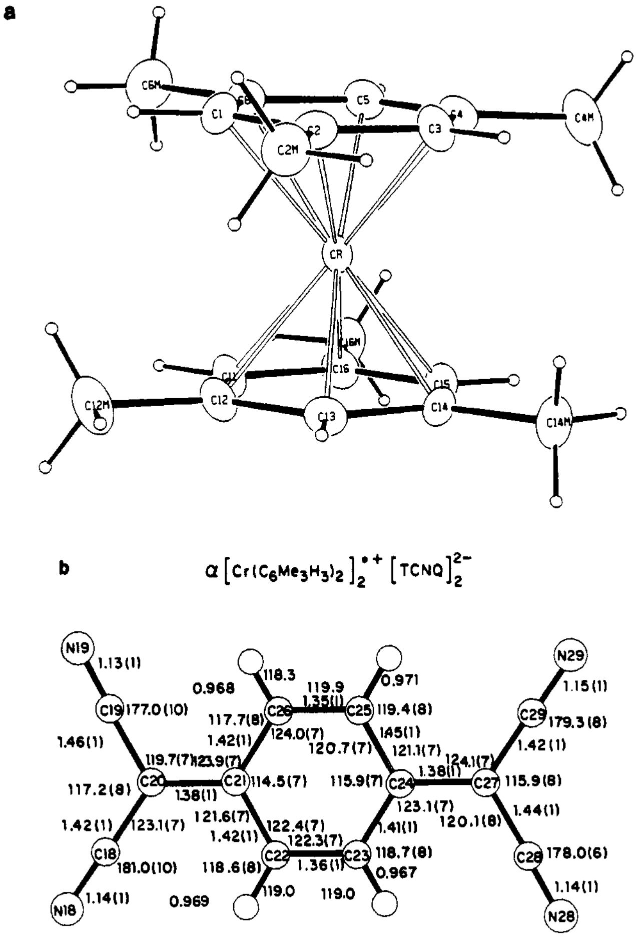

Figure 1. Atom labeling for α-$[Cr(C_6Me_3H_3)_2]^{\bullet+}[TCNQ]^{\bullet-}$, 1α.

effects were included in F_c;[17] the values for f' and f'' were those of Cromer.[16b] All calculations were performed on a Vax-11/750 computer using the SDP-PLUS package.[18]

Results and Discussion

Chemistry. The reaction of TCNQ with C_5 metallocenes can result in a variety of products.[4] The neutral bisarene transition-metal complexes with C_6 symmetry tend to be electron rich[20] and are readily oxidized by many organic cyano acceptors including TCNE[14] and TCNQ. Several TCNQ complexes with bisarene transition-metal cations including $[M(C_6Me_6)_2]^{2+}[TCNQ]_2^{2-}$ (M = Fe, Ru),[21] and $[Cr(C_6H_6)_2]^{\bullet+}$[13b,22] and $[Cr(C_6H_5Me)_2]^{\bullet+}$[13,23-25]–TCNQ complexes with 1:1[13,22] and 1:2[13b,24,25] stoichiometries have been reported. Similarly, we have found that reaction of TCNQ with $Cr(C_6Me_3H_3)_2$ or $Cr(C_6Me_6)_2$ results in $[Cr(arene)_2]^{\bullet+}[TCNQ]^-$ electron-transfer complexes. Two phases, 1α and 1β, of $[Cr(C_6Me_3H_3)_2]^{\bullet+}[TCNQ]^{\bullet-}$ were isolated and characterized. The blue-green 1α readily crystallized from methylene chloride, but the green needles of 1β were isolated only once, and further attempts at its

Table II. Positional Parameters and Their Estimated Standard Deviations for α-$[Cr(C_6Me_3H_3)_2][TCNQ]$, 1α

atom	x	y	z	B_{iso}, Å^2
Cr(1)	0.00180 (7)	0.24992 (9)	0.43797 (4)	2.63 (2)
N(18)	−0.3735 (7)	−0.0320 (5)	0.2379 (3)	6.1 (2)
N(19)	−0.3695 (7)	0.0459 (5)	0.4213 (3)	6.6 (2)
N(28)	−0.3940 (8)	0.4540 (6)	0.1327 (4)	7.1 (2)
N(29)	−0.3634 (7)	0.5352 (5)	0.3194 (3)	6.3 (2)
C(1)	0.1176 (6)	0.2151 (6)	0.5197 (3)	3.8 (2)
C(2M)	0.1251 (7)	0.0737 (6)	0.4747 (4)	4.5 (2)
C(2)	0.1250 (6)	0.1644 (5)	0.4703 (4)	3.6 (2)
C(3)	0.1319 (6)	0.2049 (6)	0.4167 (3)	3.9 (2)
C(4M)	0.1330 (7)	0.3316 (7)	0.3522 (4)	5.7 (2)
C(4)	0.1296 (5)	0.2899 (5)	0.4115 (3)	3.7 (2)
C(5)	0.1213 (6)	0.3375 (5)	0.4616 (3)	3.7 (2)
C(6M)	0.1058 (7)	0.3510 (6)	0.5679 (4)	5.2 (2)
C(6)	0.1150 (6)	0.2989 (5)	0.5156 (3)	3.4 (2)
C(11)	−0.1275 (5)	0.2834 (5)	0.4639 (3)	3.4 (2)
C(12)	−0.1244 (5)	0.1988 (5)	0.4603 (3)	3.4 (2)
C(12M)	−0.1273 (7)	0.1466 (6)	0.5135 (4)	5.2 (2)
C(13)	−0.1158 (5)	0.1614 (5)	0.4064 (3)	3.6 (2)
C(14M)	−0.0979 (7)	0.1697 (7)	0.2993 (3)	5.1 (2)
C(14)	−0.1096 (5)	0.2120 (5)	0.3563 (3)	3.5 (2)
C(15)	−0.1139 (6)	0.2967 (5)	0.3608 (3)	3.5 (2)
C(16M)	−0.1232 (7)	0.4257 (6)	0.4198 (4)	4.8 (2)
C(16)	−0.1230 (5)	0.3349 (5)	0.4142 (3)	3.4 (2)
C(18)	−0.3718 (7)	0.0200 (6)	0.2711 (4)	4.6 (2)
C(19)	−0.3676 (7)	0.0622 (5)	0.3739 (4)	4.4 (2)
C(20)	−0.3698 (6)	0.0844 (5)	0.3123 (3)	3.6 (2)
C(21)	−0.3689 (5)	0.1661 (5)	0.2967 (3)	3.3 (2)
C(22)	−0.3708 (6)	0.1907 (5)	0.2369 (3)	3.8 (2)
C(23)	−0.3717 (6)	0.2707 (5)	0.2204 (3)	4.1 (2)
C(24)	−0.3724 (5)	0.3349 (5)	0.2610 (3)	3.4 (2)
C(25)	−0.3681 (5)	0.3110 (5)	0.3221 (3)	3.4 (2)
C(26)	−0.3680 (5)	0.2314 (5)	0.3373 (3)	3.6 (2)
C(27)	−0.3760 (6)	0.4164 (5)	0.2445 (3)	3.8 (2)
C(28)	−0.3863 (7)	0.4389 (6)	0.1821 (4)	4.7 (2)
C(29)	−0.3695 (6)	0.4823 (6)	0.2857 (4)	4.1 (2)

Table III. Positional Parameters and Their Estimated Standard Deviations for β-$[Cr(C_6Me_3H_3)_2][TCNQ]$, 1β

atom	x	y	z	B_{iso}, Å^2
Cr(1)	0.000	0.000	0.000	2.38 (2)
N(8)	0.2111 (4)	0.2041 (3)	−0.3659 (6)	5.8 (1)
N(9)	0.5916 (5)	0.2818 (3)	−0.5225 (6)	6.3 (1)
C(1)	−0.2141 (4)	0.0471 (3)	−0.1255 (5)	3.35 (9)
C(2M)	−0.3299 (5)	−0.0780 (3)	−0.0370 (6)	4.6 (1)
C(2)	−0.2229 (4)	−0.0393 (3)	−0.1144 (5)	3.17 (9)
C(3)	−0.1263 (4)	−0.0870 (2)	−0.1731 (5)	3.15 (9)
C(4M)	0.0818 (6)	−0.1043 (3)	−0.3003 (6)	4.6 (1)
C(4)	−0.0231 (4)	−0.0524 (2)	−0.2425 (5)	3.04 (9)
C(5)	−0.0165 (4)	0.0343 (3)	−0.2509 (5)	3.10 (9)
C(6)	−0.1121 (4)	0.0844 (2)	−0.1937 (5)	3.08 (9)
C(6M)	−0.1025 (5)	0.1761 (3)	−0.2030 (6)	4.5 (1)
C(8)	0.3103 (5)	0.1887 (3)	−0.4098 (6)	3.9 (1)
C(9)	0.5197 (5)	0.2308 (3)	−0.4962 (6)	4.1 (1)
C(10)	0.4318 (4)	0.1669 (3)	−0.4649 (5)	3.44 (9)
C(11)	0.4671 (4)	0.0835 (3)	−0.4817 (5)	3.04 (9)
C(12)	0.5842 (4)	0.0605 (3)	−0.5414 (5)	3.36 (9)
C(13)	0.6165 (4)	−0.0196 (3)	−0.5588 (5)	3.39 (9)

---

(16) (a) Cromer, D. T.; Waber, J. T. *International Tables for X-Ray Crystallography*; The Kynoch Press: Birmingham, England, 1974; Vol. IV, Table 2.2B. (b) Cromer, D. T.; Waber, J. T. *International Tables for X-Ray Crystallography*; The Kynoch Press: Birmingham, England, 1974; Vol. IV, Table 2.3.1.

(17) Ibers, J. A.; Hamilton, W. C. *Acta Crystllogr.* **1964**, *17*, 781.

(18) Frenz, B. A. The Enraf-Nonius CAD 4 SDP-A Real Time System for Concurrent X-Ray Data Collection and Crystal Structure Determination. In *Computing in Crystallography*; Schenk, H., Olthof-Hazelkamp, R., Vankonigsveld, H., Bassi, G. C., Eds.; Delft University Press: Holland, 1978; pp 64–71.

(19) Cruickshank, D. W. *J. Acta. Crystallogr.* **1949**, *2*, 154.

(20) (a) Yur'eva, L. P.; Peregudova, S. M.; Nekrasov, L. N.; Korptkov, A. P.; Zaitseva, N. N.; Zakurin, N. V.; Vasil'kov, A. Yu. *J. Organomet. Chem.* **1981**, *219*, 43. (b) Markle, R. M.; Lagowski, J. J. *Organometallics* **1986**, *5*, 595. (c) Michaud, P.; Mariot, J.-P.; Varret, F.; Astruc, D. *J. Chem. Soc., Chem. Commun.* **1982**, 1383. (d) Finke, R. G.; Voegeli, R. H.; Laganis, E. D.; Boekelheide, V. *Organometallics* **1983**, *2*, 347. Laganis, E. D.; Voegeli, R. H.; Swann, R. T.; Finke, R. G.; Hopf, H.; Boekelheide, V. *Organometallics* **1982**, *1*, 11.

(21) Ward, M. D.; Johnson, D. C. *Inorg. Chem.* **1987**, *26*, 4231–4227.

(22) Yagubskii, E. B.; Khidekel, M. L.; Shchogelov, I. F.; Buravov, L. I.; Gribov, B. G.; Makova, M. K. *Dokl. Akad. Nauk SSSR, Ser. Khim.* **1968**, 2013–2014.

(23) Shibaeva, R. P.; Atovmyan, L. O.; Orfanova, M. N. *J. Chem. Soc., Chem. Commun.* **1969**, 1494.

(24) Shibaeva, R. P.; Atovmyan, L. O.; Ponomarev., V. I. *J. Struct. Chem.* **1978**, *16*, 792–795.

(25) Ljubovsky, R. B.; Makova, M. K.; Khidekel, M. L.; Shchogelov, I. F.; Yagubskii, E. B. *Zh. ETH Pis. Red.* **1972**, *15*, 464–465.

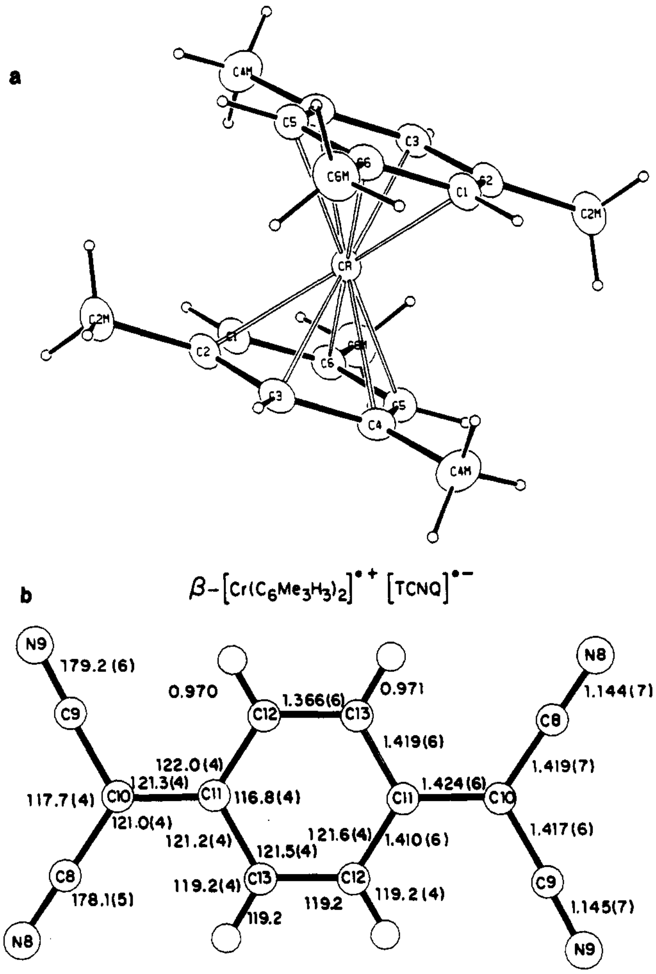

Figure 2. Atom labeling for β-$[Cr(C_6Me_3H_3)_2]^{\bullet+}[TCNQ]^{\bullet-}$, 1β.

preparation were unsuccessful. Therefore, though we were able to obtain an X-ray structural characterization of 1β, sufficient material was not available for further physical measurements.

Crystal Structure. 1α crystallizes in the monoclinic space group *C*2/*c*. The atom labeling and anion bond distances are shown in Figure 1, and Table II lists the positional coordinates. In contrast, 1β crystallizes in the monoclinic space group *P*2$_1$/*c*. The atom labeling and anion bond distances are shown in Figure 2, and Table III lists the positional coordinates.

The $[Cr(C_6Me_3H_3)_2]^{\bullet+}$ cations in both 1α and 1β are ordered with methyl groups of the two arene ligands in a mutually staggered conformation. The internal bond distances and angles are similar to those reported previously for the $[Cr(C_6H_6)_2]^{\bullet+}$[13a,26] and $[Cr(C_6H_5CH_3)_2]^{\bullet+}$.[13a,23-25] The Cr–C, C–C, and C–Me separations are in the ranges 2.141 (6)–2.173 (8), 1.38 (1)–1.44 (1), and 1.49 (1)–1.54 (1) and average 2.154, 1.41, and 1.51 Å, respectively, for the α-phase. For the β-phase the Cr–C, C–C, and C–Me separations are in the ranges 2.147 (4)–2.172 (4), 1.406 (6)–1.426 (6), and 1.501 (7)–1.509 (7) and average 2.161, 1.414, and 1.506 Å, respectively. The Cr–C$_6$(ring) centroids for both phases are 1.63 Å.

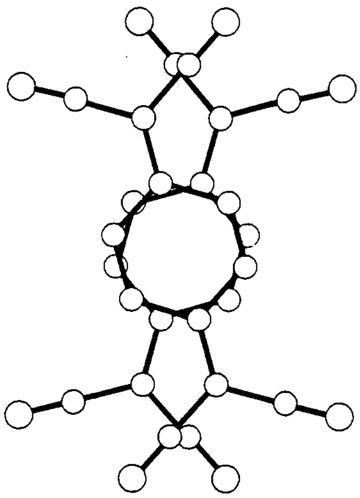

Figure 3. Structure of the $[TCNQ]_2^{2-}$ dimer in α-$[Cr(C_6Me_3H_3)_2][TCNQ]$, 1α.

The $[TCNQ]^{\bullet-}$ anions in the α-phase exist as $[TCNQ]_2^{2-}$ dimers, which exhibit a different structure than previously reported. The distances and angles are presented in Figure 1, bottom. $[TCNQ]_2^{2-}$ dimers have been previously reported, e.g., Rb[TCNQ],[27] $Cs_2[TCNQ]_3$,[28] $\{[Fe(C_5Me_5)_2]^{\bullet+}\}_2[TCNQ]_2^{2-}$,[6,29] and $[M(C_6Me_6)_2]^{2+}[TCNQ]_2^{2-}$ (M = Fe, Ru).[21] The previuosly characterized dimers exhibit slipped eclipsed conformations where slippage occurs either along the short, **3a**, or along the long TCNQ axis, **3b**. An unusual staggered conformation, **3c**, is observed for the $[TCNQ]_2^{2-}$ dimer in 1α, wherein the ring centroids are collinear with the chain axis, but the dihedral angle between the planes normal to the long molecular axes of the individual anions is 31°, Figure 3. The methyl groups of the cation appear to interact with the TCNQ's in a cog arrangement, and this possibly leads to the large dihedral angle. Additionally, the intradimer separation of 3.47 Å is substantially longer than the 3.10 Å observed for $[TCNQ]_2^{2-}$ (**3b**) in $\{[Fe(C_5Me_5)_2]^{\bullet+}\}_2[TCNQ]_2^{2-}$ [29] or the 3.21-Å separation in $[M(C_6Me_6)_2]^{2+}[TCNQ]_2^{2-}$ (M = Fe, Ru).[21] Thus, it is not surprising that the ν(C≡N) infrared spectra of 1α possesses absorptions (2152 s and 2175 s cm^{-1}) more characteristic of the isolated $[TCNQ]^{\bullet-}$ {cf. 2152 s and 2179 s cm^{-1} for $[Fe(C_5Me_5)_2]^{\bullet+}[TCNQ^{\bullet-}]$[8b] than the $[TCNQ]_2^{2-}$ dimer (vide infra). All chemically equivalent bond distances are within 2 standard deviations of being equal.

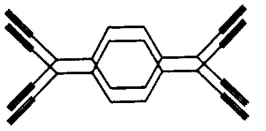

3a

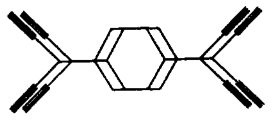

3b

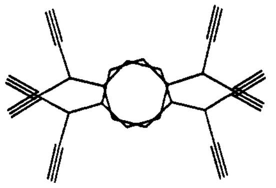

3c

The salt 1α possesses 1-D chains containing dimer dianions sandwiched between the two adjacent [Cr-

---

(26) (a) Shibaeva, R. P.; Shvets, A. E.; Atovmyan, L. O. *Dokl. Akad. Nauk. SSSR* **1971**, *199*, 334. Morosin, B. *Acta. Crystallogr., Sect. B* **1974**, *30*, 838.

(27) Hoekstra, A.; Spoelder, T.; Vos, A. *Acta Crystallogr., Sect. B* **1972**, *28*, 14.

(28) Fritchie, C. J., Jr.; Arthur, P., Jr. *Acta Crystallogr., Sect. B* **1966**, *21*, 139.

(29) Reis, A. H., Jr.; Preston, L. D.; Williams, J. M.; Peterson, S. W.; Candela, G. A.; Swartzendruber, L. J.; Miller, J. S. *J. Am. Chem. Soc.* **1979**, *101*, 2756.

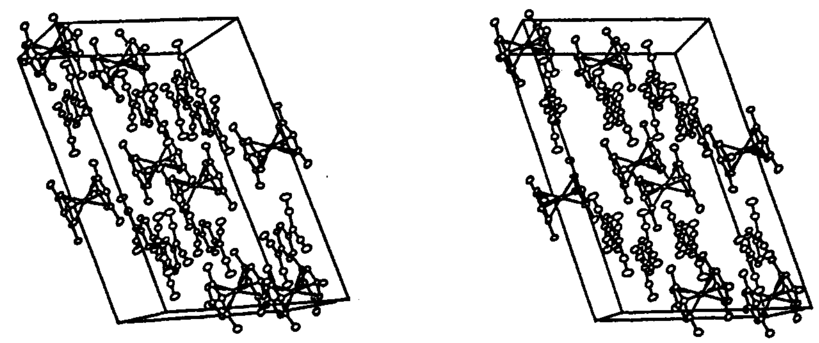

Figure 4. Stereoview of the unit cell of α-$[Cr(C_6Me_3H_3)_2][TCNQ]$, **1α**.

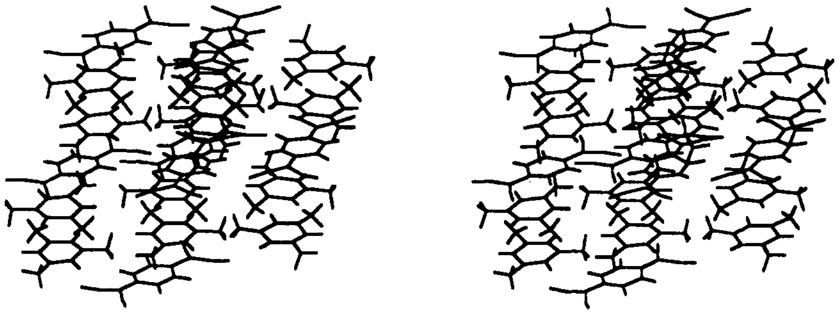

Figure 5. Stereoview of the unit cell of β-$[Cr(C_6Me_3H_3)_2][TCNQ]$, **1β**.

$(C_6Me_3H_3)_2]^{\bullet+}$ cations in a $\cdots D^{\bullet+}D^{\bullet+}A_2^{2-}D^{\bullet+}D^{\bullet+}A_2^{2-}\cdots$ arrangement, Figure 4. Although also observed for $[Cr(arene)_2]^{\bullet+}[TCNE]^{-}$,[14] this motif is not commonly observed for TCNQ complexes and has only been reported previously for complexes in which the cations are linked by a cyclophane ligand in $[(C_5Me_5)_2Ru_2(2_2\text{-}[4,4']\text{-}cyclophane)]^{2+}[TCNQ]_2^{2-}$.[30] The anion and arene planes within a given stack are slightly tilted by 6° with respect to each other. The anion–cation separation of 4.03 Å reflects minimal electronic interactions and is substantially longer than the ~3.5 Å observed for the anion–C_5 ring separation for $[Fe(C_5Me_5)_2]^{\bullet+}$ [A = TCNQ, TCNE, $C_4(CN)_6$, and DDQ].[4] The cations adjacent to each other within a stack are separated by 3.43 Å with intrachain Cr···Cr separations of 6.680 and 14.126 Å and interchain Cr···Cr separations of 8.365 and 8.618 Å.

The β-phase possesses isolated $S = {}^1/_2$ $[TCNQ]^{\bullet-}$ similar to that reported for $[Fe(C_5Me_5)_2]^{\bullet+}[TCNQ]^{\bullet-}$.[6] The distances and angles are presented in Figure 2, bottom. The distances and angles are very close to those observed previously for $[TCNQ]^{\bullet-}$.[6] This phase consists of 1-D $\cdots D^{\bullet+}A^{\bullet-}D^{\bullet+}A^{\bullet-}\cdots$ chains of alternating $S = {}^1/_2$ $[TCNQ]^{\bullet-}$ anions and $S = {}^1/_2$ $[Cr(C_6Me_3H_3)_2]^{\bullet+}$ cations, similar to the metamagnetic phase of 1:1 $[Fe(C_5Me_5)_2]^{\bullet+}[TCNQ]^{\bullet-}$,[6] Figure 5. The intrachain Cr···Cr separation is 10.772 Å while the Cr···N separations are 6.126, 6.784, 7.514, and 8.025 Å. The interchain separations are 8.419, 9.213, and 9.588 (Cr···Cr), 3.951, 4.336, and 4.470 Å (N···N), and 5.250, 5.266, 5.329, 6.755, and 9.324 (Cr···N). The anion–cations separation of 3.50 Å is typical of the van der Waals separation.

Although the lack of suitable single crystals of **2** prevented the determination of the structure by X-ray methods, the $\nu(C{\equiv}N)$ infrared spectrum of **2** provides partial information concerning the arrangement of the anions. Sharp $\nu(C{\equiv}N)$ absorptions are observed at 2156 m, 2175 s, and 2182 s cm^{-1}. These are characteristic of $[TCNQ]_2^{2-}$ [cf. 2157 m, 2176 s, and 2184 s cm^{-1} for $\{[Fe(C_5Me_5)_2]^{\bullet+}\}_2[TCNQ]_2^{2-}$, where the $[TCNQ]_2^{2-}$ dimer has an arrangement as in **3b** and an interplanar separation of 3.10 Å].[29] Thus, the solid-state motif is tentatively identified as either 1-D $\cdots D^{\bullet+}A_2^{2-}D^{\bullet+}D^{\bullet+}A_2^{2-}D^{\bullet+}\cdots$ or an isolated herringbone $D^{\bullet+}A_2^{2-}D^{\bullet+}$ arrangement as both are observed in $[Fe(C_5Me_5)_2]^{\bullet+}$ salts of $[TCNQ]^{\bullet-}$.[6]

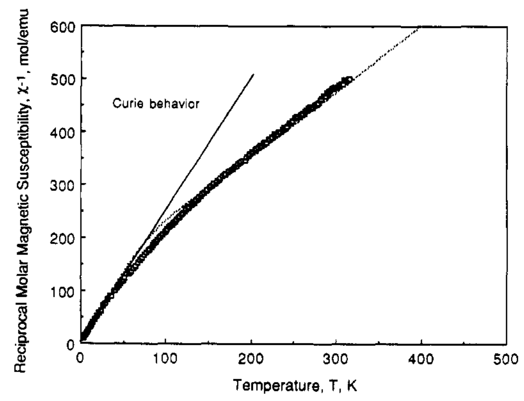

Figure 6. Inverse molar magnetic susceptibility as function of temperature for **1α**. Equation 1 is plotted as a dotted line.

Magnetic Properties

Magnetic Susceptibility. The magnetic susceptibilities of **1α** and **2** were measured between 2 and 320 K by the Faraday method. The susceptibility of **2** obeys the Curie–Weiss law, $\chi_M = C/(T - \theta)$ with an effective moment, μ_{eff}, of 1.77 μ_b and θ of −0.1 K. This is consistent with the expectation of 1.73 μ_B for one independent spin per repeat unit and the infrared spectrum which indicates the presence of the diamagnetic $[TCNQ]_2^{2-}$ dimer.

In contrast, the susceptibility of **1α** does not obey the Curie–Weiss law, Figure 6a. The effective moment, μ_{eff}, monotonically increases from 1.73 μ_B at 2.3 K to 2.34 μ_B at 320 K, Figure 6b. At low temperatures the value of the molar susceptibility is consistent with only one independent spin contributing to the susceptibility. As described above, **1α** possesses dimers with a 3.47-Å interplanar separation. The susceptibility reflects antiferromagnetic coupling of the spins on adjacent anions with a

---

(30) Chestnut, D. B.; Arthur, P., Jr. *J. Chem. Phys.* **1962**, *36*, 2969.

singlet ground state and an energetically accessible triplet excited state. At low temperature only $[Cr(C_6Me_3H_3)_2]^{\bullet+}$ contributes to the magnetic susceptibility. However, with increasing temperature the susceptibility increases over the single spin value and can be understood in terms of two independent contributions arising from the paramagnetic $[Cr(arene)_2]^{\bullet+}$ cation (simple Curie–Weiss law) and thermal population of the triplet excited state of the $[TCNQ]_2^{2-}$ dimers. The data can be fit by eq 1, where N

$$\chi = \underset{\text{singlet–triplet term, }[\mathrm{TCNQ}]_2^{2-}}{[2Ng^2\mu_B^2/3k_BT]/[1 + \exp(\Delta E/k_BT)/3]} + \underset{\text{Curie-Weiss term, }[\mathrm{Cr(Arene)_2}]^{\bullet+}}{[Ng^2\mu_B^2]/[3k_B(T - \Theta)]} \qquad (1)$$

is Avrogadro's number, k_B is the Boltzmann constant, μ_B is the Bohr magneton, g is the Lande' g factor, and ΔE is the energy of the singlet–triplet gap. The first term on the right side describes the singlet–triplet behavior for $[TCNQ]_2^{2-}$ dimers, and the second term the simple Curie-Weiss contribution from the cation. The best fit to the data is ΔE = 315 K (0.027 eV, 219 cm^{-1}, 0.44 kcal/mol) and θ = 0 K for **1**α.

Numerous complex TCNQ electron-transfer salts in which the average number of excess electrons per TCNQ is less than one {e.g., $[Cs^+]_2[TCNQ]_3^{2-}$,[30] $[Ph_3PMe]^+$-$[TCNQ]_2^-$,[31] and $[(C_5Me_5)_2Ru_2(2_2\text{-}[4,4']\text{-cyclophane})]^{2+}$-$[TCNQ]_4^{2-}$[32]} are known to exhibit energetically accessible triplet excited states. However, $[TCNQ]_2^{2-}$ dimers with geometries **3a** and **3b** generally are so strongly coupled that population of the triplet state is not readily observed at reasonable temperatures. We note that $[Cr(C_6H_5Me)_2]$-[TCNQ] exhibits strong antiferromagnetic coupling between $[TCNQ]^{\bullet-}$ anions, as determined from magnetic susceptibility and ^1H NMR spectra.[13b] Thus, the observation of spin exchange in **1**α is unusual. We attribute this unusually small spin exchange energy to the atypical TCNQ ring–ring overlap, depicted as **3c**, and the rather large interplanar separation in the dimer. This overlap apparently does not allow strong spin pairing that occurs with the more conventional ring-over-ring or ring-over-bond overlaps.[33]

Electron Paramagnetic Resonance. The EPR spectra of $[Cr(arene)_2]^{\bullet+}$ as the $[PF_6]^-$ salt is typical with g = 1.987.[34] Solutions of **1** or **2** in CH_2Cl_2 at room temperature exhibit isotropic signals with g = 1.995 (ΔH_{pp} = 11.2 G) presumably due to the overlap of signals from $S = {}^1/_2$ $TCNQ^{\bullet-}$ and $Cr(C_6Me_3H_3)_2^{\bullet+}$ ions. Neither ^{15}N nor ^{53}Cr hyperfine coupling are resolvable.

Powdered samples of **1**α at room temperature exhibit two overlapping isotropic resonances centered at g = 1.988 with ΔH_{pp} = 29 G. As the temperature is lowered to 110 K, one of the signals splits into a doublet with a splitting of 9.2 G. The two signals observed at room temperature may be explained by an isotropic signal for the $^2A_{1g}$ $[Cr(C_6Me_3H_3)_2]^{\bullet+}$ cations superimposed on a exchange-broadened triplet resonance due to thermal population of the triplet S = 1 excited state for the $[TCNQ]_2^{2-}$ dianion.

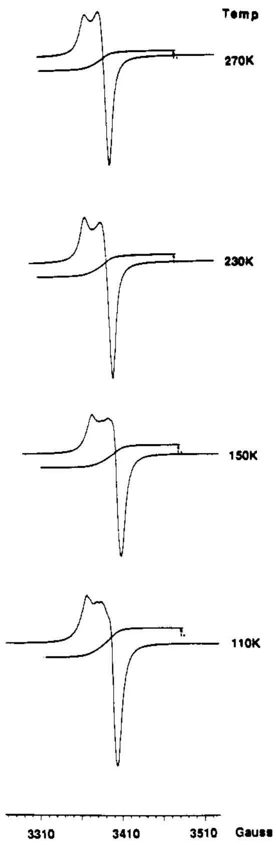

Figure 7. Powder EPR spectra of at crystalline **1**α at 110, 150, 230, and 270 K.

As the temperature is lowered, the number of populated triplet states decreases and dipolar-induced zero-field splitting becomes resolvable, Figure 7. Unfortunately the spectra were never sufficient for more detailed analysis of the triplet fine structure. The $\Delta m_s = \pm 2$ transition at half-field characteristic of triplet states in organic solids[35] was not observed above 110 K. However, its absence may be due to the factors such as exchange broadening, which remove the dipolar splitting at higher temperatures, which in turn removes the dipolar-induced mixing of states that relieves the forbiddeness of the $\Delta m_s = \pm 2$ transition. At lower temperatures where the dipolar splitting begins to emerge, the triplet state may not be populated sufficiently for its observation.

Acknowledgment. We thank W. R. Bachman, E. Delawski, E. Matthews, S. McLean, D. Wipf, and C. Vazquez for their technical assistance.

Registry No. 1, 126859-54-9; 2, 130010-97-8.

Supplementary Material Available: Summary of the crystallographic data, tables of bond distances and angles, least-squares plane, anisotropic thermal parameters, and general temperature factors for the α- and β-phases of $[Cr(C_6Me_3H_3)_2][TCNQ]$ (20 pages); tables of calculated and observed structure factors (22 pages). Ordering information is given on any current masthead page.

---

(31) Chestnut, D. B.; Phillips. W. D. *J. Chem. Phys.* **1961**, *35*, 1002.

(32) Ward, M. D.; Fagan, P. J.; Calabrese, J. C.; Johnson, D. C. *J. Am. Chem. Soc.* **1989**, *111*, 1719–1732.

(33) Endres, E. In *Extended Linear Chain Compounds*; Miller, J. S., Ed.; Plenum Press: New York, 1983, Vol. 1, pp 263–317.

(34) Fitch, J. W., III; Lagowski, J. J. *Inorg. Chem.* **1965**, *4*, 864–867.

(35) Wasserman, E.; Snyder, L. C.; Yager, W. A. *J. Chem. Phys.* **1964**, *41*, 1763. Wertz, J. E.; Bolton, J. R. *Electron Spin Resonance, Elementary Theory and Practical Applications*; Chapman and Hall: New York, 1986; p 249.